Int J Earth Sci (2000) 89 : 90–107

ORIGINAL PAPER

R. Scherreiks

Platform margin and oceanic sedimentation in a divergent and convergent plate setting (Jurassic, Pelagonian Zone, NE Evvoia, Greece)

Received: 25 June 1999 / Accepted: 30 November 1999

Abstract The carbonate formations of NE Evvoia, Greece, are remnants of the mature terrace phase of a shelf that evolved, from the Late Triassic through the Late Jurassic, on the periodically slumping passive margin of the Pelagonian micro-continent, initially in a divergent and later in a convergent setting. A starved shelf configuration is indicated by northward, distal thinning (<200 m) and deepening of facies, in contrast to southward, proximal thickening (>1000 m) and shallowing of facies. Tectonic subsidence dictated the deposition of the generally deepening-upward facies succession, which begins with peritidal carbonates and ends with radiolarites and siliciclastic turbidites. However, recurrent shallowing upward cycles show that carbonate accumulation also responded to oscillating sea level. The large-scale shelf architecture consists of three sequences: a progradational highstand tract, a shelf margin tract and a transgressive tract. The transgressive sequence was initiated in a convergent setting by tectonic loading and ended during approximately the Latest Jurassic with the emplacement of an (Eohellenic) ophiolite nappe over the Pelagonian formations. Contemporaneous with the deepening-upward succession of the Pelagonian margin, a shallowing-upward succession formed on top of the oceanic ophiolite assemblage, initially below the CCD in the early divergent setting, later above the CCD in the convergent setting.

Key words Hellenides · Pelagonian Eohellenic microfacies · Palaeoenvironments · Basin evolution · Tectonic mélange · Ophiolite emplacement

R. Scherreiks
Geologische Staatssammlung, Luisenstrasse 37, D-80333 Munich, Germany
Tel.: +49-89-21806520
Fax: +49-89-21806514
e-mail: rudolph.scherreiks@iaag.geo.uni-muenchen.de

Introduction

Palaeogeographically, the study area in NE Evvoia, Greece (Fig. 1), is a part of the Pelagonian zone of the Hellenides, a micro-continent upon which a carbonate platform evolved adjacent to deeper marine zones: the externally located Subpelagonian and Pindos zones, and the internally located Vardar zone (Aubouin 1959, 1965; Guernet 1971; Jacobshagen et al. 1978a). Rapid subsidence of the Pelagonian platform during the Late Jurassic foreshadowed the tectonic emplacement of the Eohellenic ophiolite nappe (Bernoulli and Laubscher 1972; *Eohellenic* after Jacobshagen et al. 1976 for the ophiolites emplaced on top of the Pelagonian zone formations in the Late Tithonian to Early Cretaceous), of which the ophiolite complex of NE Evvoia is a small erosional remnant (Baumgartner and Bernoulli 1976). The palaeogeographical origin of the Eohellenic ophiolite, whether from the Vardar or from the Pindos ocean, is still controversial (e.g. Mercier 1966; Bernoulli and Laubscher 1972; Dercourt 1972; Hynes et al.1972; Zimmerman 1972; Smith et al. 1975; Zimmerman and Ross 1976; Jacobshagen et al. 1978a; Smith et al. 1979; Mountrakis et al. 1983; Robertson 1991; cf. Scherreiks 1998b; Clift 1998). However, the ophiolite obduction led to cessation of the Jurassic carbonate depositional cycle in the Pelagonian zone.

The formations of northern Evvoia have been previously mapped as time-stratigraphic units (Katsikatsos et al. 1980), but microfacies analysis data are still very scarce (Scherreiks 1998a). The present paper focuses on the lateral and vertical facies associations of the preserved tectonostratigraphic assemblages, and on basin architecture (Ingersoll and Busby 1995), prior to the time of ophiolite emplacement. The petrogenesis of the ophiolite and a full-scale tectonic analysis are beyond the scope of this paper, but the palaeogeographic relations of the platform margin to the overthrust oceanic sedimentary succession and to the ophi-

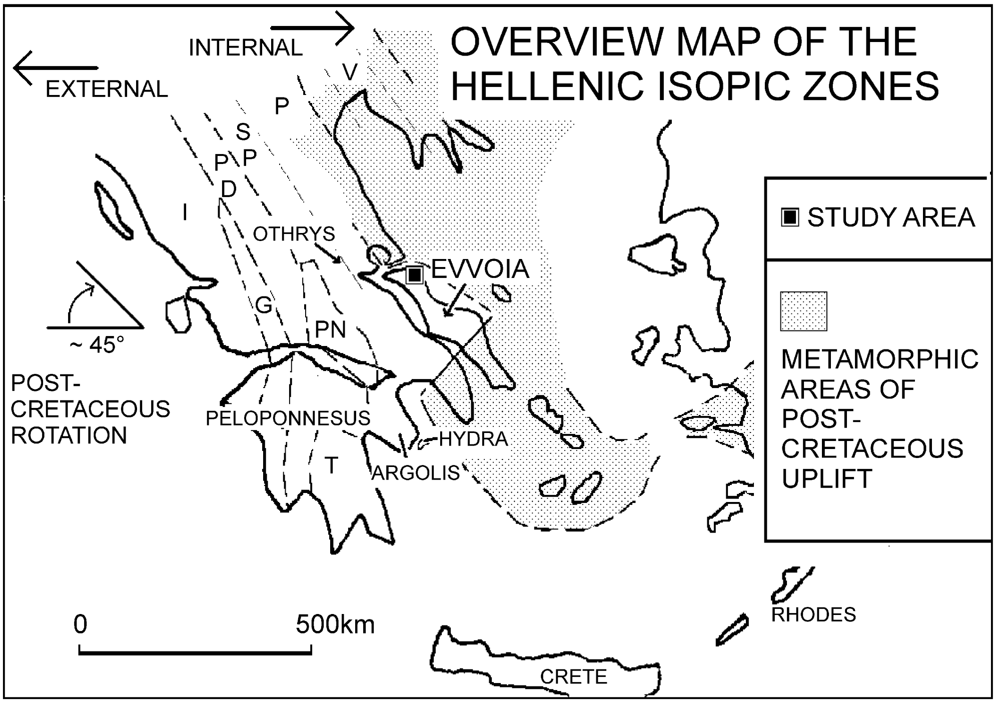

Fig. 1 Overview map of the Hellenic isopic zones. The study area in NE-Evvoia is located in the Pelagonian isopic zone (Aubouin 1959), which is non-metamorphic in the study area, in contrast to major exhumed areas located to the east, north and south. The sense of post-Cretaceous rotation (Kissel and Laj 1988) and the isopic zones are shown. V Vardar; P Pelagonian; SP Subpelagonian; PD Pindos; PN Parnasos; G Gavrovo; T Tripolitza; I Ionian

olite assemblage and mélange have been assessed, whereby post-Eohellenic rotations (McKenzie and Jackson 1986; Kissel and Laj 1988) and regional palaeogeography (Stampfli et al. 1998) have been taken into consideration.

Field work was carried out from 1993 to 1997, over 250 samples and over 230 thin sections were studied, and 392 fabric measurements were evaluated (Schmidt net density distributions, Pangaea Scientific 1998). Chemical analyses were carried out on selected laterites, lateritic rocks, and Fe-Mn crusts (ICP: ISA-Instruments, Lyon, France).

Geological overview

The formations of the study area belong to two different palaeogeographic and tectonostratigraphic units: the non-metamorphic Pelagonian zone formations (Katsikatsos et al. 1986), herein referred to simply as the Pelagonian formations, and the Oceanic formations, which are of controversial origin.

Amongst the Pelagonian formations, a northern and a southern facies zone has been distinguished (Figs. 2, 3): the relatively thick (>1000 m) mainly peritidal, neritic, reefal to hemipelagic succession, in the south, contrasts with the comparatively thin (<200 m) mainly hemipelagic to pelagic succession, in the north. A hemipelagic palaeoenvironment was maintained throughout most of the Jurassic in the northern zone while peritidal and neritic conditions persisted in the south, until the entire area (north and south) was drowned below the CCD during the Late Jurassic, as is shown by the sudden appearance of carbonate-free radiolarites. The Pelagonian formations are mainly of Jurassic age (Table 1; Katsikatsos et al. 1980) except for a reefal intraformational breccia of ?Permotriassic (Katsikatsos et al. 1980) to Upper Triassic age (Robertson 1991), located east of Ellinika. The Permotriassic and older basement is exposed outside of the

Table 1 The fossils of the Xiron Foramation (reef and neritic debris limestones; in corroboration with O. Ebli and F. Schlagintweit)

Protopeneroplis striata WEYNSCHENK: Middle to Upper Jurassic (cf. p. C741–42, Moore 1964)
Parakilianina rahonensis (FOURY and VINCENT) Kimmeridgian (cf. Flügel 1974; Figs. 2, 3, 4, 6, Table 1)
Parurgonina caeinensis CUVILLIER, FOURY and PIGNATTI MORANO: Oxfordian to Portlandian
Haurania sp. aff. deserta HENSON: Jurassic (cf. Moore 1964, p C492–C493)
Thaumatoporella parvovesiculifera RAINERI: (cf. Flügel 1974 Taf. 3/3)
Cladocoropsis mirabilis FELIX: Kimmeridgian (cf. Hudson 1953; Hanzawa 1961, Pl. LXXIV; Flügel 1974, Taf. 2/1)
Actinostromaria tokadiensis YABE and SUGIYAMA: Kimmeridgian (cf. Turnsek and Barbulescu 1969, Pl. 1)
Actinostromarianina cf. lecomptei HUDSON: (cf. Hudson 1955, Pl. XXII/6)
Parastromatopora sp.: (cf. Hanzawa 1961 Pl. LXXIV; Hashimoto 1960, Pl. 1/1,2)
Milleporidium sp.
Lithocodium sp.
Bacinella irregularis RADOICIC
Rivulariacea nodule (Cayeuxia): (cf. Flügel 1974, Pl. 28/3; Perconig 1968, Pl. XC/2; and Cita 1965, Pl. XIII/2)
Zergabriella embergeri (BOUROULLEL and DECOFFRE) GRANIER: Tithonian? Berriasian/Valanginian

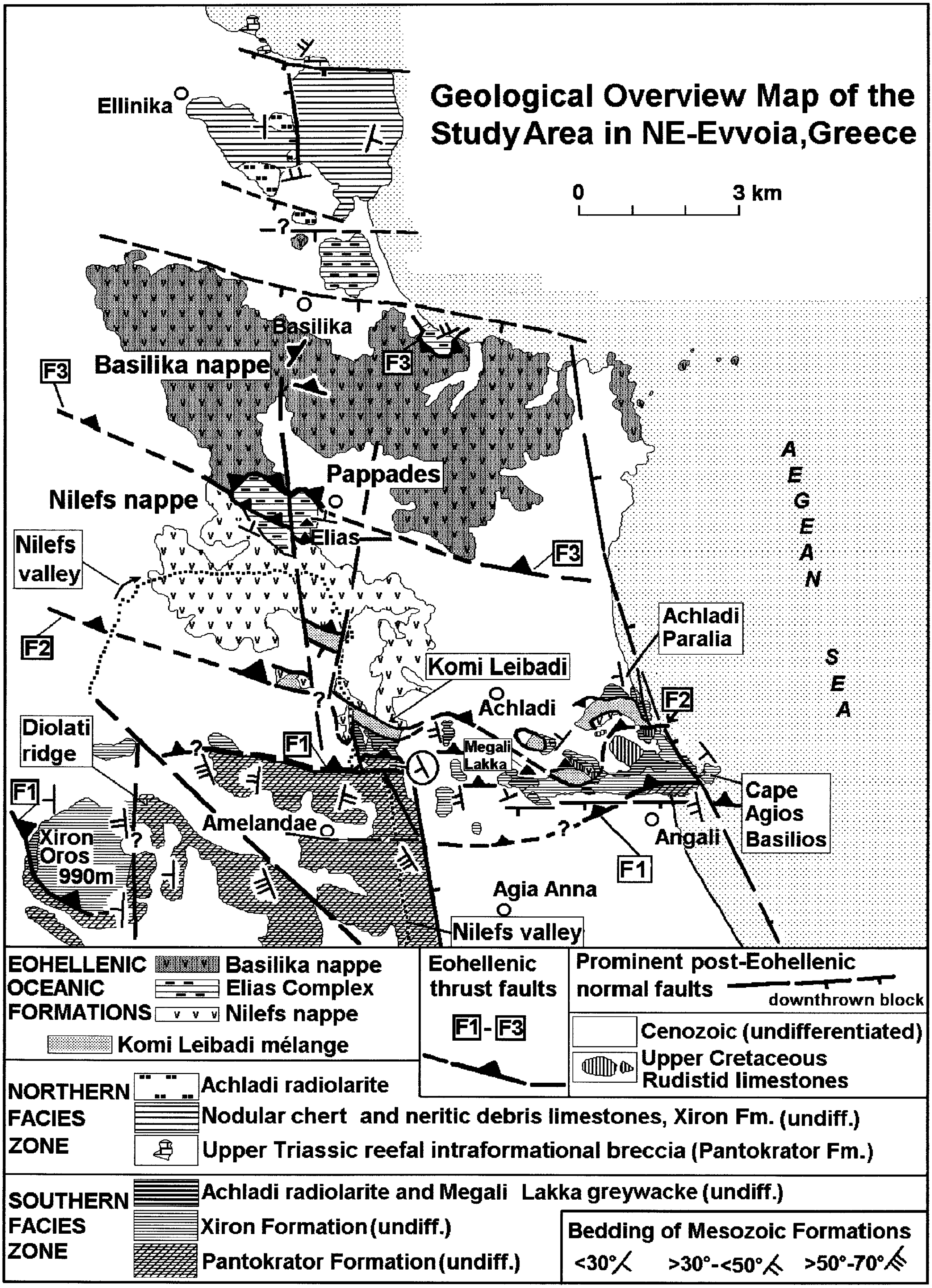
Geological Overview Map of the Study Area in NE-Evvoia, Greece
0 3 km
Ellinika
Basilika
Basilika nappe
F3
Pappades
Nilefs nappe
Elias
Nilefs valley
F2
Achladi Paralia
Komi Leibadi
Achladi
Diolati ridge
F1
Megali Lakka
Amelandae
Xiron Oros 990m
Angali
Cape Agios Basilios
Agia Anna
Nilefs valley
AEGEAN SEA
EOHELLENIC OCEANIC FORMATIONS
Basilika nappe
Elias Complex
Nilefs nappe
Komi Leibadi mélange
Eohellenic thrust faults
F1-F3
Prominent post-Eohellenic normal faults
downthrown block
Cenozoic (undifferentiated)
Upper Cretaceous Rudistid limestones
NORTHERN FACIES ZONE
Achladi radiolarite
Nodular chert and neritic debris limestones, Xiron Fm. (undiff.)
Upper Triassic reefal intraformational breccia (Pantokrator Fm.)
SOUTHERN FACIES ZONE
Achladi radiolarite and Megali Lakka greywacke (undiff.)
Xiron Formation (undiff.)
Pantokrator Formation (undiff.)
Bedding of Mesozoic Formations
<30°
>30°-<50°
>50°-70°

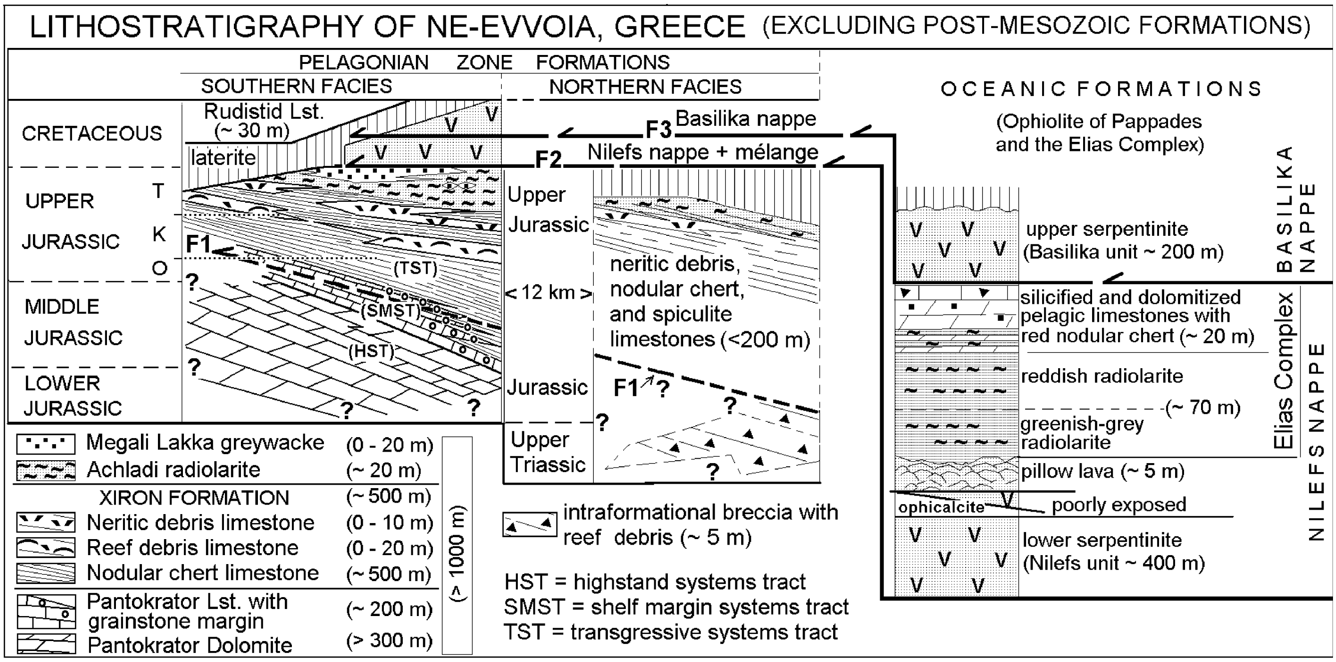

Fig. 3 Lithostratigraphy of the Mesozoic formations of NE Evvoia. Two Hellenic Isopic zones are represented in the study area: the Pelagonian zone and an oceanic isopic zone of disputed origin. The Pelagonian zone facies in the southern part of the study area consist of a relatively thick succession of peritidal dolomites, neritic limestones, hemipelagic carbonates with reef-debris and neritic debrite intercalations, radiolarites and greywackes. In contrast to this, the northern part of the study area consists of a condensed succession of Jurassic deeper water facies and a tectonically disconnected Upper Triassic reefal intra-formational breccia (Robertson 1991; cf. {Katsikatsos et al. 1980). The position of interpreted, large-scale sequence tracts are shown. The Ophiolite of Pappades and the pelagic facies of the Elias Complex are oceanic formations, whichcompose a composite nappe (Eohellenic ophiolite). The restored lateral relations and the positions of the major thrust faults are indicated (F1, F2, F3)

Table 2 The fossils of the Rudistid limestone, Prasidi area (in corroboration with O. Ebli and F. Schlagintweit)

Basal beds
Hippurites sp.: (Turonian-Maastrichtian)
Radiolitidae: (Cretaceous)
Planorbulina cretae (Marson): on a rudistid clast (Coniacian)
Uppermost beds
Idalina sp. (aff. I. antiqua SCHLUMBERGER and MUNIER-CHALMAS): Senonian (cf. Moore 1964 p. C470–472)
Plummerita bronnimanni (aff. P. hantkeninoides BRÖNNIMANN): Maastrichtian (cf. Moore 1964, p. C662–C663)
Rotaliacea: Upper Cretaceous – Recent (Moore 1964)

immediate study area (15 km west and ca. 5 km north; Katsikatsos et al. 1984).

The oceanic formations of controversial origin consist of tectonically emplaced mélange, ophiolite and a pelagic sedimentary complex deposited on the ophiolite substrate (Figs. 2, 3). The ophiolite is an Eohellenic ophiolite (Jacobshagen et al. 1976), emplaced on top of the Pelagonian zone formations in the Late Tithonian to Early Cretaceous (cf. Baumgartner and Bernoulli 1976).

Regional uplift followed ophiolite emplacement (Bernoulli and Laubscher 1972) and was accompanied by Lower Cretaceous erosion, karstification, and the deposition of Fe-rich and Al-poor laterite deposits in fractures, karstic vugs and breccias, and as pisolith crusts over the post-Eohellenic unconformity. The laterites were found to contain anomalous Ni, Cr and Co, substantiating a post-Eohellenic ophiolitic provenance (cf. Melidonis 1960; Guernet 1965; Kurzweil 1966; Katsikatsos et al. 1969; Spiliadis 1977). A pre-Eohellenic emersion surface with bauxites, of upper Middle to lower Upper Jurassic age like that of central Evvoia (Guernet and Robert 1973), could not yet be verified in the study area. However, considering that the Pappades Ophiolite was tectonically loading the Pelagonian margin during its late Middle Jurassic advance (see later discussion), a plausible consequence could have been emersion of the Pelagonian hinterland.

◀

Fig. 2 Geological overview map of the study area in NE Evvoia. The geological map is based on the latest IGME Geological Map (1980, Limni Sheet, 1:50,000) and own mapping and reconnaissance of mainly the pre-Cenozoic areas at the scales 1:25,000 and 1:5000 during the years 1993 to 1997. The detailed mapping was done in the triangle between Cape Agios Basilios, Xiron oros and Elias. Although the Mesozoic formations are covered to a great extent by Cenozoic clastic deposits, almost complete north–south and east–west sections are nevertheless exposed (compare Fig. 4). The tectonically emplaced Eohellenic oceanic formations of the central area cover the Pelagonian formations. Bedding attitudes, and major faults are shown. Location names are referred to in the text

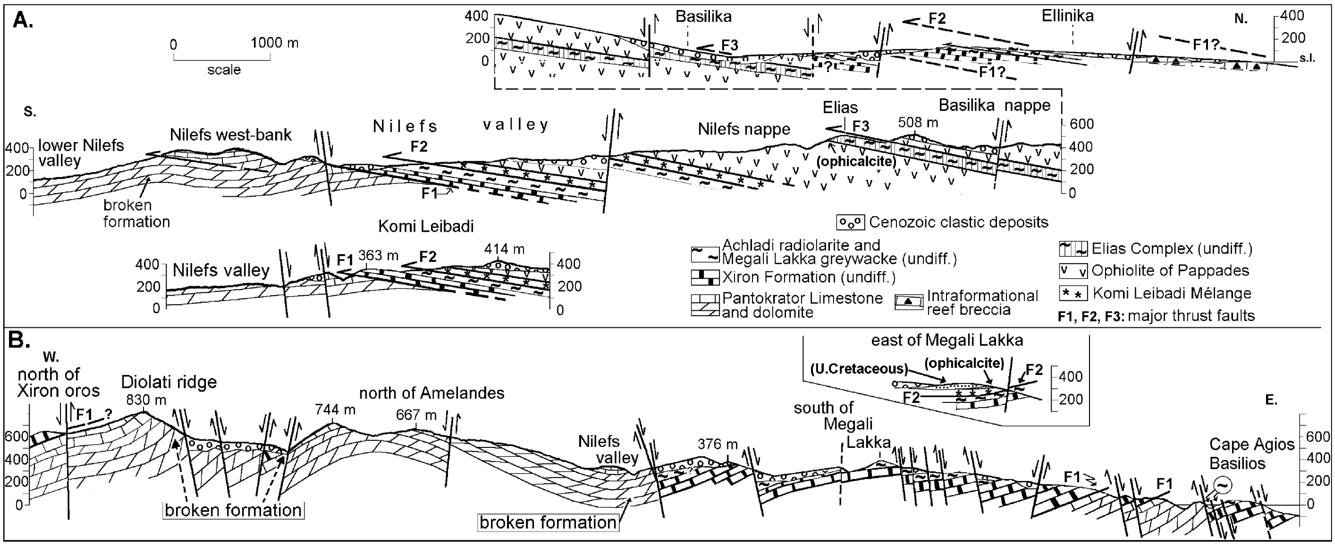

Fig. 4A,B Geological sections. **A** The north–south section between Ellinika and the lower Nilefs valley and the inset with a parallel section through the Komi Leibadi area show the large-scale stratigraphic and structural situation. The major thrust faults (F1, F2, F3) are south-vergent and a tectonic mélange is found between the ophiolite composite nappe and the greywacke and radiolarite of the southern part of the study area. The youngest tectonic event was normal faulting. **B** The east–west section, between Cape Agios Basilios and Xiron oros, and the parallel section east of Megali Lakka, show in particular the superposition of post-Upper Cretaceous structures related to major Cenozoic events: folding and westward tilting of the Mesozoic formations (compare Fig. 8); uplift, erosion, and sedimentation; normal faulting (see Diagram 1 of Fig. 7); renewed erosion

The first reliably dated Post-Eohellenic marine sedimentation is documented in the study area by rudistid limestones (Chenevart and Katsikatsos 1967), which are widespread in the Hellenides (Renz 1955; Aubouin and Guernet 1964; Guernet 1965; Bignot et al. 1971; Katsikatsos 1977). They occur southeast of Achladi (Fig. 2), are up to approximately 30 m thick, and range in age from about Coniacian to Maastrichtian (Table 2).

The terrestrial Cenozoic formations (Katsikatsos et al. 1980; Katsikatsos et al. 1981), which were deposited on the uplifted and eroded Mesozoic substrate, exhibit steep normal and strike-slip faults (Fig. 4B; cf. McKenzie and Jackson 1986). In the present paper, the post-Eohellenic (post-ophiolite emplacement) deformations have been investigated only so far as to distinguish them from Eohellenic deformations.

The Pelagonian formations

The Pelagonian formations consist of: the Pantokrator Formation (Pantokrator Dolomite and Limestone); the Xiron Formation (nodular chert limestone, reef debris limestone, neritic debris limestone); the Achladi radiolarite; and the Megali Lakka greywacke (Fig. 3).

The Pantokrator Formation

The peritidal carbonates at the base of the stratigraphic column are assigned to the Pantokrator Formation in this paper. Until now, they have been informally distinguished as "Middle Triassic–Upper Jurassic limestones and dolomites" (Aubouin and Guernet 1964; Guernet 1965; Katsikatsos 1976, 1977; Katsikatsos et al. 1986). Although the type-locality of the Pantokrator Limestone (*Pantokratorkalk*) is the Pantokrator massif of northeast Korfu (Partsch 1887; Flügel 1983), this formation nevertheless has a wide regional distribution, extending from Korfu into the Parnasos and Pelagonian zones (Renz 1955; Bannert and Bender 1968; Bachmann and Risch 1979; Schäfer and Senowbari-Daryan 1982; Baumgartner 1985; Jacobshagen 1986). The Pantokrator Limestone is typically diachronous with dolomitic lithofacies, so that Bernoulli and Renz (1970) informally distinguished "Pantokrator Dolomite" from "Pantokrator Limestone", a distinction which will be followed here.

The Pantokrator Dolomite crops out mainly between the Nilefs valley and the Xiron massif and a small outcrop is near Angali (Fig. 2), but does not occur in the northern facies zone (Fig. 3). It is dark grey, massive to well bedded (15 cm to 2 m), weathers grey to light grey, and is occasionally stained red by iron hydroxides. Pervasively dolomitized fenestral stromatolite, intraclast stromatolite and pisolith-grainstone are typical. Large bodies of the Dolomite, mainly near the base, have been deformed into broken formation (Fig. 4; Hsü 1974). The Pantokrator Dolomite is approximately 300 m thick and is laterally transitional and covered by the Pantokrator Limestone (Figs. 3, 4).

The Pantokrator Limestone crops out mainly between the Xiron Oros and the Diolati ridge, and in smaller exposures along the southern part of the Nilefs valley (Fig. 2). It is dark grey to brownish grey, usually well bedded (10–50 cm), and occasionally laminated. Typical facies are cross-bedded oolites and molluscan rudstones and floatstones containing megalodonts and gastropods. Occurrences of *Thaumatoporella parvovesiculifera* (RAINERI) are reminiscent of the Pantokrator Limestone of Korfu (Flügel 1983) and of Hydra (Schäfer and Senowbari-Daryan 1982). These Pantokrator Limestone facies occur only in the southern facies zone. However, an intraformational breccia, containing reef-debris, only occurring in the northern facies zone (Figs. 2, 3), is considered here to be equivalent to the Pantokrator Limestone. As Robertson (1991) points out, it is probably of Late Triassic age and may document platform slumping related to early platform rifting and basal clastic deposition.

The Pantokrator Limestone is approximately 200 m thick (Figs. 3, 4). Towards the top, a thick (25–50 m) succession of cross-bedded oolites occurs, which is laterally associated and intercalated with mudstone and nodular-spiculite wackestone (Xiron Formation).

Palaeoenvironments and basin architecture of the Pantokrator Formation

The microfacies of the Pantokrator Dolomite give a fairly precise palaeobathymetry for this part of the stratigraphic column: The dissolution fenestrae contain crystal silts and limpid drusy, zoned dolomite-spar cements, which indicate freshwater vadose to mixed-water phreatic environments (Land 1973; Folk and Land 1975; Ward and Halley 1985; Humphrey 1988). Vadose environment is substantiated by the meniscus cements (Dunham 1971) in *Pisolith dolo-rudstones*, which have also been described in the Pantokrator Formation of other areas (cf. Schäfer and Senowbari-Daryan 1982; Flügel 1983). Widespread *Laminoid fenestral stromatolites* (dolo-boundstone), having laminoid to hemispheroidal and porostromate fabrics of probable cyanobacterial origin (Monty 1981), complete the picture of an extensive supratidal to intertidal palaeoenvironment. The microfacies with dissolution fenestrae or meniscus cements indicate subaerial exposure, and such facies reoccur cyclically in the Pantokrator Dolomite (see below). Early diagenetic "mixing-zone" type dolomitization (Hanshaw et al. 1971; Badiozamani 1973), is thought to have prevailed, particularly because signs of hypersalinity are completely lacking, and the excellent preservation of fabrics suggests that dolomitization took place near the surface before compaction and cementation substantially reduced permeability (Sibley 1982; Sibley and Gregg 1987). *Packed peloid dolo-mudstone to wackestone* is a common microfacies, consisting of bioturbated micrite and peloids with occasional micro-bioclasts, interpreted to represent intertidal back-beach lagoonal environments.

The shelly to micritic microfacies of the Pantokrator Limestone are interpreted to represent palaeoenvironments ranging from barrier beaches to a distal

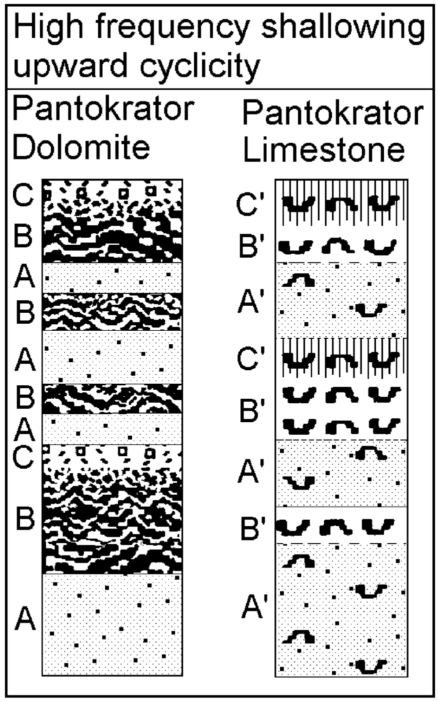

Fig. 5 Shallowing upward cyclicity. High-frequency third- to fifth-order cyclicity in the 1- to 2-m range occurs in the limestone and dolomite members of the Pantokrator Formation. Ideal cycles in the Pantokrator Dolomite consist of: A pelleted dolo-mudstone, 40–220 cm; B stromatolite (dolo-boundstone), 50–200 cm; C vadose fenestral stromatolite and dolo-pisolite with meniscus cement, 5–20 cm. Ideal cycles in the Pantokrator Limestone consist of: A' bioclast floatstone, 10–150 cm; B' bioclast rudstone, 20–100 cm; C' vadose bioclast rudstone showing selective aragonite dissolution and calcite cement, less than 1 m

neritic terrace. *Rudaceous molluscan packstones* and *floatstones*, containing thick-shelled molluscan clasts and biomorphs (megalodonts and high spired gastropods: Nerineids and Cerithiids), are envisioned to have built up beaches and fore slopes. Alternating phreatic/vadose influence is documented by recurring horizons in which the shells have been organically coated and micritized, whereas in others they have been dissolved and subsequently cemented in two generations with an initial isopachous layer of scalenohedral calcite followed by pore-occluding rhombohedral calcite (Fig. 5). A more distal subtidal terrace is most likely represented by *Peloid bioclast wackestones* and *packstones*, composed of peloids and varying amounts of micrite lumps, cortoids, *Thaumatoporellid* clasts, articulated and disarticulated ostracods, textularians and miliolinids. Imbricate shelly beds are indicative of high-energy episodes on this neritic terrace.

The maintenance of near supratidal environments, during the period in which the Pantokrator Formation attained a thickness of over 500 m, indicates that tectonic subsidence as well as Jurassic global sea-level rise (second-order Zuni cycle; Sloss 1963; Hallam 1988) were fully compensated by the carbonate sedimentation. Typical for the Pantokrator Formation are high-frequency third- to fifth-order asymmetric shallowing-upward cycles in the 1- to 2-m range, usually culminating with subaerial exposure (Fig. 5). Cycles like these have been observed in the Pantokrator Formation of Hydra and the Argolis peninsula (Schäfer and Senowbari- Daryan 1982) and extend throughout the western Liassic Tethys (Bosence et al. 1999), demonstrating their regional significance. High-frequency shallowing upward peritidal cycles have been explained by allocyclicity (see Fischer 1986; Plint et al. 1992; Schulz and Schäfer-Neth 1997) as well as autocyclicity (see reviews in Grotzinger 1986 and Pratt et al. 1992), whereas rapid tectonic ups and downs are considered improbable (Plint et al. 1992). The observed Pantokrator 1- to 2-m cycles can have been caused either by eustacy or intrinsic (autocyclic) processes of carbonate sedimentation or both, superimposed on a generally subsiding platform.

On the whole, the Pantokrator Formation built up a prograding, periodically shoaling platform, which, in the terminology of sequence stratigraphy (Sarg 1988; Van Wagoner et al. 1988), can be interpreted as a high-stand systems tract (HST), characterised by proximal peritidal and distal neritic terrace facies. The Pantokrator HST is succeeded by a 25- to 50-m-thick package of oolitic grainstones (micritized tangential ooids and composite ooids), interpreted as an equilibrating shelf marginal wedge systems tract (SMST; after Sarg 1988). Drusy calcite-spar-cements indicate that this marginal wedge probably was temporally exposed. Toward the top, the oolites intercalate with and are eventually covered by deeper-water facies (Xiron Formation).

Age-range of the Pantokrator Formation

Regional comparisons indicate that the Pantokrator Formation of the study area ranges in age from approximately Late Triassic to Upper Jurassic (cf. Katsikatsos 1976 , 1977; Katsikatsos et al. 1980, 1986). The intraformational reefal breccia of the northern facies zone (Figs. 2, 3), being of probable Late Triassic age (Robertson 1991), was coeval with the Late Triassic to Early Jurassic reefs of Hydra (Schäfer and Senowbari- Daryan 1982).

Xiron Formation

The Xiron Formation consists of three main lithofacies, considered here as informal formations: nodular chert limestone; reef-debris limestone; and neritic debris limestone (Fig. 3). The latter two debris limestones are conventionally grouped together as "*Cladocoropsis* limestone" (Renz 1955; Flügel 1974; Jacobshagen 1986), but are considered here as two distinct lithofacies.

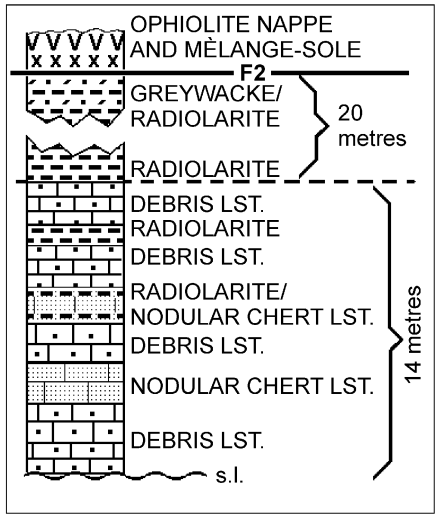

Fig. 6 The Xiron Formation/Achladi radiolarite transition at Achladi beach. The upper 14 m of the Xiron Formation, at Achladi beach, is a transition of interstratified neritic debris limestones and nodular chert limestones, intercalated carbonate-free radiolarite in nodular chert limestones, and finally interdigitated debris limestones in radiolarite

The Xiron Formation is laterally transitional with and transgresses over the oolitic grainstones that form the final succession of the Pantokrator Formation, and in turn is covered by the Achladi radiolarite (Figs. 3, 6). In the northern facies zone, the Xiron Formation has an exposed composite thickness of less than 200 m; in the south it is 500 m thick (Figs. 3, 4).

Nodular chert limestone comprises the major part of the Xiron Formation. It has been described previously in Evvoia (Guernet 1965; Katsikatsos et al. 1980; Katsikatsos et al. 1986; Robertson 1991), and a similar lithofacies is widespread in the Hellenides (Renz 1955; Jacobshagen 1986). The nodular chert limestone is a dark-grey to black, bituminous, porcelainous-micrite, sporadically containing nodular chert. Bedding is most often not well developed. Intercalations of *Cladocoropsis*-bearing reef limestones appear in the upper third part of the nodular chert limestone. A very similar 200- to 300-m succession of bituminous limestones with oolites near the base and *Cladocoropsis* limestone progressively higher up has been described by Robertson (1991) in central Evvoia.

Reef debris limestone

"*Cladocoropsis* limestone" and "*Cladocoropsis* Zone" (Turnsek et al. 1981) are informal and formal usage for a widespread reefal limestone known to extend from the Apennines, through the Dinarides and Hellenides into the Near East and also to Japan (Hanzawa 1961; Sartoni and Crescenti 1962; Flügel 1974; Turnsek et al.1981). Turnsek et al. (1981) interpret the *Cladocoropsis* Zone as a sheltered back reef area of a reef complex, comparable to the present Great Barrier Reef of Australia. In the study area and elsewhere it is characterised by an array of hydrozoans, notably *Cladocoropsis* mirabilis FELIX, in addition to other frame-builders and encrusting algae (Flügel 1974). *Cladocoropsis* bearing limestones appear to be limited to the Internal Hellenides (Fig. 1), extending from the vicinity of the study area to the Peloponnesus, Crete, Rhodes, and Cyprus (Renz 1940, 1955; Celet 1962; Mutti et al. 1970; Bassoulet and Guernet 1970; Guernet 1971; Jacobshagen et al. 1978a; Dercourt et al. 1980; Rimpel and Rothenhöfer 1983). This facies has not been reported in the External Hellenides (Smith et al. 1975; stratigraphic overview in Jacobshagen 1986).

In the study area, reef debris limestone (=*Cladocoropsis* limestone in the strict sense) is composed of rudaceous reefal components and lithoclasts derived from framestones, containing macroscopically discernible frame-builders (Table 1). The intergranular pores were occluded by organic crusts, fibrous cement, silty-micritic sediment, and lastly by drusy calcite spar. The latter cement indicates late diagenetic vadose conditions. Reef debris limestone occurs in beds of 1–20 m, intercalated in nodular chert limestone, and is found only in the southern facies zone (e.g. Cape Agios Basilios, Megali Lakka, and Xiron Oros; Fig. 2).

Neritic debris limestone is a turbiditic facies (Baumgartner and Bernoulli 1976), occurring interstratified with nodular chert limestone and radiolarite in the top 14–20 m of the Xiron Formation (Fig. 6). This facies is distinguished from the reefal debris facies by its lateral association with radiolarites and great variety of allochems comprising echinoids, crinoids, molluscs, foraminifera, bryozoans, ostracods, algal lithoclasts, peloids, micritized ooids, quartz-silt, seldom hydrozoans, including *Cladocoropsis*, stromatoporids, scleractinians, and admixtures of monaxone spicules and radiolarians. The relatively thin intercalations of medium to fine-arenitic neritic allochems in the northern facies zone have been tectonically flattened and sheared, whereas in the south, the debris is generally coarser and the intercalations thicker.

Palaeoenvironments and basin architecture of the Xiron Formation

The depositional environments of the Xiron Formation extended seaward from shallow neritic oolite banks (SMST) of the Pantokrator Formation to a deeper neritic terrace, composed of spiculite wackestones, containing calcareous peloids, siliceous monaxone and tetraxone spicules, calcispheres, few radiolarians and forams; and transported, micritized ooids. Calcareous spicules and minor detrital quartz are less common. This terrace transgressed over the SMST during approximately the Middle Jurassic, and during the Late Jurassic it was studded with photic zone algal-encrusted hydrozoan patch reefs, which occasionally may have been subaerially exposed (pore-occluding silt and calcite cement). Reef debris, consisting of pebble to boulder-size clasts (up to 80 cm across; Robertson 1991), accumulated either in the vicinity of the patch reefs or at the base of syngenetic fault escarpments along the terrace margin. Direct observation of such faults have not been made, but evidence for their one-time existence is given by intercalations of reefal and other neritic debrites in radiolarites (see Achladi radiolarite) which are in close proximity, in time and space, with the reef debris facies (Fig. 6). Therefore, beyond the terrace a rapidly deepening, slumping carbonate mud slope, composed mainly of spiculite mud and diagenetic chert nodules, is envisaged to have extended down below the CCD level where terrace-derived neritic debris and spiculite mud interdigitated with radiolarite. A metalliferous layer in the northern facies zone (Robertson 1991) can be regarded as a hardground of a starved environment. This (H. Bahlburg, pers. commun.) could be strongly indicative to rapid deepening after tectonic loading. The basin architecture is envisioned to have been a developing tectonically depressed foreland basin (cf. Ingersoll and Busby 1995) that thinned toward the northern facies zone (Fig. 3).

In the context of sequence stratigraphy (Sarg 1988), where the Xiron Formation stratigraphically succeeds the SMST of the Pantokrator Formation, a transgressive systems tract (TST) begins. The large scale changeover from a HST (see Pantokrator Formation), to an equilibrating SMST, to a TST is interpreted as the response of carbonate accumulation to the changeover from divergent to convergent plate polarity. This is referred to later and in the Discussion.

Age

The Xiron Formation ranges in age from Upper Triassic to Upper Jurassic (Katsikatsos et al. 1980). However, in the northern facies zone, the Xiron Formation is in still problematic tectonic contact with Late Triassic Pantokrator intraformational reef-debris breccia (Robertson 1991). The typical Tethyan reef facies of the upper part of the Xiron Formation (*Cladocoropsis* limestone; Flügel 1974) ranges in age from Oxfordian to approximately Tithonian, shown by *Parurgonina*, the suite of hydrozoans (cf. Bassoulet and Guernet 1970; Flügel 1974, 1982), and the calcareous alga *Zergabriella* (Table 1) found in the neritic debris limestone.

Achladi Radiolarite and the Megali Lakka Greywacke

A much-investigated radiolarite formation, which is widespread in the Hellenides, outcrops at Achladi Paralia (Fig. 2; la série radiolaritique: Guernet and Parrot 1972; Baumgartner and Bernoulli 1976; Robertson 1991). It has been informally referred to as the Achladi radiolarite and has been described in detail by Baumgartner and Bernoulli (1976): it is a succession of radiolarian silts and mudstones, radiolarian cherts, with sporadic laminae of graded lithic arenite; at the base it is laterally transitional with neritic-debris facies; it is approximately 20 m thick, and it is in contact with a so-called boulder bed, which actually is an ophiolite mélange. This contact is a transition from coherent bedded radiolarite, to sheared radiolarite and to tectonic mélange on top (see below Komi Leibadi mélange).

Lateral and vertical associations

In the south, the radiolarite intercalates with nodular chert and neritic-debris limestones (Figs. 3, 6). In the northern facies zone (near Ellinika; Fig. 4A) the radiolarite is tectonically imbricated with nodular-chert and neritic debris limestones. Intercalations of turbiditic lithic sandstones of minor thickness occur toward the top of the sequence at Achladi beach (Baumgartner and Bernoulli 1976). These graded and laminated lithic arenites were described by Robertson (1991) as an example of the widespread "quartzose flysch" facies also found in central Evvoia, the Pindos and Subpelagonian zones (Jones et al. 1992). In some locations (Megali Lakka, Nilefs Valley) the thicknesses of these lithic sandstones (greywackes) swell on to noteworthy sheets and lenses (Scherreiks 1998a). They are of siliciclastic greywacke lithology, occurring near and at the top of the Achladi radiolarite in lenses that attain up to 20 m thickness, having tens of metres width, and up to a few hundred metres length (Megali Lakka, Komi Leibadi, Nilefs valley). However, the original thickness of the greywacke is not known because of tectonic offscraping, which must have taken place as is shown by the abundant greywacke components in the superposed tectonic mélange (Figs. 3, 4, 6).

Lithology

The quartzose greywackes are of the lithic to feldspathic types (Folk 1965), consisting of relatively high percentages (10–20%) of feldspar and lithic grains and having a very fine clayey-micaceous matrix, comprising well over 15% and up to approximately 40–50% of the groundmass. Most grains (80–90%) are quartz, either unstrained mono-crystalline or, to a lesser extent, stressed and showing undulose extinction. The weathered feldspar grains consist of orthoclase, albite-twinned plagioclases, few simple-twinned orthoclases, and rare microcline. The lithic grains consist of polycrystalline sutured quartzite with undulose extinction, quartz sandstone, chert and granitic lithic grains. Some opaque grains and mica-flakes of sand size occur also. A search for dolomite lithic-grains was negative and neither calcite nor limestone lithoclasts could be found, which was verified by staining the thin sections with alizarin-red-s. The typical turbidites exhibit flat, uniform bedding, typical fining-upward grading, convolute laminations and occasional ripple marks. Textural immaturity is shown by moderate to poor sorting, a wide range of angular to rounded grains, and low to high sphericities.

Palaeoenvironments of the Achladi radiolarite and the Megali Lakka Greywacke, and basin architecture

The relatively sudden appearance of mainly green-grey, occasionally red, radiolarites, devoid of calcite, indicate that the Pelagonian carbonate shelf substrate subsided below the concomitant CCD, into a generally starved, poorly oxygenated environment, where initially the radiolarian ooze, carbonate turbidites, and debris flows accumulated. Later, long after carbonate deposition ceased, turbiditic lithic sands (cf. Robertson 1991), were deposited prior to the tectonic emplacement of the Pappades Ophiolite and Komi Leibadi mélange (see below). The mineralogy of the greywackes resembles the granitic composition of the Pelagonian basement (e.g. exposed 5 km north and 15 km northeast of the study area), suggesting that an uplifted block of Pelagonian basement was the likely source of the Megali Lakka Greywacke. The lack of carbonate in the greywackes indicates that the transporting medium probably did not pass over the carbonate shelf, and the lack of volcanic or ophiolitic grains in the greywackes precludes oceanic provenance. The siliciclastic laden turbidity currents were most likely transported parallel to the shelf slope from a distal source of uplifted Pelagonian basement, a common phenomenon during collisional events (Ingersoll et al. 1995). The ESE–WNW strike of the long axis of a greywacke lens in the area of Komi Leibadi may represent the orientation of the Pelagonian shelf margin and possibly a foredeep, which has been suggested by Robertson (1991) to have developed in front of the Hellenic ophiolite prior to its obduction. The turbiditic greywacke and the radiolarite were the final deposits before the emplacement of the Ophiolite of Pappades and Komi Leibadi mélange.

Age of the Achladi radiolarite and Megali Lakka Greywacke

Based on the radiolarian assemblage, Baumgartner and Bernoulli (1976) ascertained a Tithonian to Valanginian, probably a Berriasian to Valanginian age for the Achladi radiolarite. De Wever (in Ferrière et al. 1989) and Robertson (1991) assign a Kimmeridgian to Tithonian age to stratigraphically corresponding radiolarites outside of the present study area. The neritic debris limestone at the base of the radiolarite sequence, at Achladi beach, is of Tithonian age or younger, indicated by the alga *Zergabriella embergeri* (Table 1), so that the superposed 20 m thick radiolarite and greywacke formations must be of the order of *later* Tithonian or younger, which supports an age close to that originally suggested by Baumgartner and Bernoulli (1976).

The Oceanic formations

The Elias Complex and its substrate, the Ophiolite of Pappades are of controversial oceanic provenance (Eohellenic ophiolite; see Introduction). These units were tectonically emplaced over the Pelagonian formations together with the Komi Leibadi mélange.

The Pappades Ophiolite

The Pappades Ophiolite forms a 100-km^2 massif in the centre of the study area (Figs. 2, 3, 4A). It is a remnant of Eohellenic ophiolite (Jacobshagen et al. 1976; for definition see Introduction), like the petrographically similar ophiolite complex of central Evvoia (Bèbien et al. 1980). The Pappades Ophiolite gained some attention for the magnesite occurring in post-Cretaceous fractures (Petrascheck 1961; Katsikatsos et al. 1975).

The ophiolite assemblage

In adherence to the Penrose-conference definition (Anonymous 1972), the Pappades Ophiolite is an incomplete, dismembered, ophiolite assemblage, which is only approximately 500 m thick. Pillow basalts lie on top of a thin layer of ophicalcite, which in turn is on top of the main bulk of the ophiolite, a serpentinite, petrographically similar to the ophiolite of central Evvoia, which has harzburgite composition (cf. Capedri 1974; Bèbien et al. 1980), with some lherzolite bodies (Parrot and Guernet 1972). The normally to be expected sheeted dyke, gabbroic and cumulate complexes (Spray 1991) are missing. The pelagic succession of Elias lies on top of the pillow lavas.

Nappe structure

The Pappades Ophiolite has an imbricate internal structure in which two main nappes have been distinguished: the Nilefs and Basilika ophiolite nappes (Figs. 2, 3, 4A). The Nilefs nappe, together with the tectonic mélange (Komi Leibadi) lies on top of the Achladi radiolarite and Megali Lakka greywacke formations (thrust fault F2: Fig. 4A). The Basilika ophiolite nappe rests on top of the Nilefs ophiolite nappe and the pelagic Elias Complex (thrust fault F3). The composite thickness of both nappes is approximately 1000 m, showing that the Pappades Ophiolite has been drastically reduced in thickness compared with other ophiolites and oceanic crust (numerous authors in Spray 1991). Small outcrops of ophicalcite, occurring at the base of ophiolite-*klippen* (southeast of Achladi; Figs. 2, 4B) and below the pillow lavas, may have formed by the hydrothermal alterations along faults or in the vicinity of sea-floor vents near faults (cf. Capedri 1974; Lavoie 1995).

Elias Complex

The Elias Complex is a radiolarite–dolomite–limestone succession, exposed in tectonic windows west of the village of Pappades and east and north of Basilika (Figs. 2, 3, 4A). This Complex is distinguished from the Achladi radiolarite because it has a strikingly different lithology and because it occurs on top of an oceanic substrate, the pillow lavas of the Pappades Ophiolite, a distinction not made previously (Katsikatsos et al. 1980). The Elias Complex is approximately 60–100 m thick and consists, from bottom to top, of radiolarian cherts and pelites, inter-laminated radiolarite and dolomitized limestone, dolomitized nodular-chert limestone, and strongly silicified pelagic limestone. The greenish-grey radiolarian pelite, overlying the pillow lava, gradually reddens upwards. Towards the top of the complex, centimicron- to centimetre-scale red chert and dolomite laminae appear, which are succeeded by 10 m of wavy bedded dolomites containing red chert nodules. The dolomites are laterally associated with dark-grey, strongly neomorphosed and silicified limestones. The complex is tectonically overlain by the Basilika ophiolite nappe (Figs. 3, 4A).

Palaeoenvironments

The radiolarites, which are devoid of carbonate, were deposited in an oceanic realm below CCD on top of pillow lavas. Intercalations of intraclasts (0.2–4 mm) on top of recurring scoured surfaces and millimetre ferruginous-manganiferous crusts (0.73–9.6% Fe and 580 ppm – 0.18% Mn), indicate periods of submarine erosion and, respectively, periods of non-deposition (hardgrounds). The chert-nodule dolostone at the top of the succession is composed of clear sucrose, euhedral dolomite, intercrystalline ferruginous matter and seldom preserved siliceous radiolarians and spicules. This is a dolomitized pelagic limestone, in which the chert-nodules were probably formed from the silica of former radiolarians and spicules. The query as to the origin of the dolomite is beyond the scope of the present study, but examples of deep-sea dolomite are not unusual (i.e. Kelts and McKenzie 1984; Mullins et al. 1985).

The upward colour change of the radiolarian pelites from green-grey to red, and the gradual appearance of pelagic carbonates in their stead (Fig. 3), most probably resulted from ocean-floor uplift into better oxygenated and above-CCD environments. This uplift could have occurred during an early stage of thrusting as the Nilefs-nappe (Figs. 2, 3, 4) ophiolite substrate was advancing towards the Pelagonian margin (Scherreiks 1998a) before it was emplaced during Late Tithonian/Early Cretaceous; thus, the upper part of the Elias Complex may have formed in a piggyback-type basin (cf. Ori and Friend 1984).

Age

Like the Achladi radiolarite which was overthrust by the Nilefs nappe during approximately Late Tithonian/Early Cretaceous, the Elias Complex was overthrust by the Basilika nappe, suggesting that it is of similar age. The lower part has not yet been dated.

Fig. 7 Tectonic data in pole diagrams. Diagram 1: Faults in the Cenozoic formations (post-Eohellenic). Most of the faults strike about NW–SE and dip either E or W at angles over 70°. Smaller maxima represent strikes and dips of ca. 180°/40°E, 80°/90°, 90°/90°, and 80°–100°/40°–60°S. These faults are readily distinguished from the Eohellenic thrust fault maximum (compare Diagrams 2a,b). Diagrams 2a,b: Faults and shear in the Jurassic Pelagonian formations, between Xiron Oros and Cape Agios Basilios. Diagram 2a depicts all faults dipping >50°, and matches well with Diagram 1, indicating that these steeply dipping faults are, by and large, post-Eohellenic, Cenozoic faults. Diagram 2b depicts all faults dipping <50°. The distinct maximum represents the present attitude of the Eohellenic thrust faults, striking and dipping around 84°/18° NNW, which do not occur in the Cenozoic formations. Diagram 3a: Bedding of the Pelagonian formations between Xiron Oros and Cape Agios Basilios. The strike and dip of the bedding maximum is 353.3°/33° WSW. Diagram 3b depicts this maximum rotated −45°, restoring pre-Cenozoic palaeogeographic North (PN). Diagram 3c shows the bedding maximum after two rotations: R1=−45° around a vertical axis and R2=a rotation of 33° SSW around a horizontal axis striking 308.3°, restoring original horizontality. Diagram 4a: Thrust faults and shear in the Elias Complex and adjacent ophiolite nappes. This maximum corresponds to a strike and dip of 70°/17° NNW. Diagram 4b: rotation R1 shifts the data to a maximum at 25°/17° WNW. Diagram 4c: rotations R1 plus R2 shifts the data to a maximum at 98°/33° NNE.
Diagram 5a: Thrust faults and shear in the Jurassic Pelagonian formations (same as Diagram 2b). Diagram 5b: rotation R1 shifts the strike and dip maximum to 39°/18°NW. Diagram 5c: after rotations R1 and R2, the maximum is at 98°/37° NNE

The Komi Leibadi Mélange

The Komi Leibadi Mélange has variable thickness up to approximately 25 m, occurring in the vicinity of Komi Leibadi and in a few other areas (Figs. 2, 4). It is in tectonic contact over the Pelagonian radiolarite and greywacke formations, and is covered by the Nilefs ophiolite nappe. This tectonostratigraphic position shows that it is genetically related to the Pagondas Complex of central Evvoia, defined by Robertson (1991, p 27, 29) as: "... a mélange of pervasively broken lithologies with a matrix"; a unit occurring between the Mesozoic platform of the Pelagonian zone and "a major ophiolite above". This mélange has an extensive distribution in the Internal Hellenides (Mercier and Vergely 1972; Parrot and Guernet 1972; Baumgartner and Bernoulli 1976; Spray and Roddick 1980; Simantov and Bertrand 1987; Ferrière et al. 1989). However, the Pagondas mélange of central Evvoia is a "polygenetic mélange" (Robertson 1991), consisting of volcaniclastics, serpentinite, shallow- and deep-water limestones, radiolarian chert, matrix supported conglomerates (i.e. diamicrit; Robertson 1991), sandstone and shale, in addition to kilometre-sized sheets and blocks of neritic limestone, and metre to tens-of-metre-scale fragmented sheets (i.e. broken formation; Robertson 1991). The lithology of the Komi Leibadi mélange is remarkably different: it does not contain limestones, diamicrit, nor kilometre-size broken formation.

The quasi-broken formations in the northern facies zone, south of Ellinika, have been considered by Robertson (1991) to be part of the Pagondas Complex. An investigation of these formations shows them to consist of Xiron Formation lithofacies covered by Achladi radiolarite, which, contrary to the coeval equivalents in the southern facies zone, have undergone strong tectonic shear, imbrication, and ductile deformation. Despite this advanced stage of deformation, these formations are identified as a contiguous stratigraphic succession; thus, they are not considered to be part of the Pagondas Complex in this paper.

Lithology

The Komi Leibadi mélange is composed of matrix supported lozenge-shaped autoclasts (Hsü 1974) of radiolarite, greywacke, basaltic lava and altered glass, serpentinite, amphibolite and anorthosite. The matrix is clayey-arenitic and was derived mainly from sheared radiolarite and greywacke. House-size autoclasts are composed of serpentinite, amphibolite and anorthosite. An amphibolite block of approximately 100 m in diameter is located at Komi Leibadi, and a large phacoid of saussuritized anorthosite (ca. 125 × 20 m) occurs east of Megali Lakka (Fig. 2). The mélange exhibits a stacked structure (Scherreiks 1998a), with predominantly greywacke clasts and few volcaniclasts at the base, in contrast to a higher content of volcaniclasts and the appearance of amphibolite, anorthosite and serpentinite toward the top.

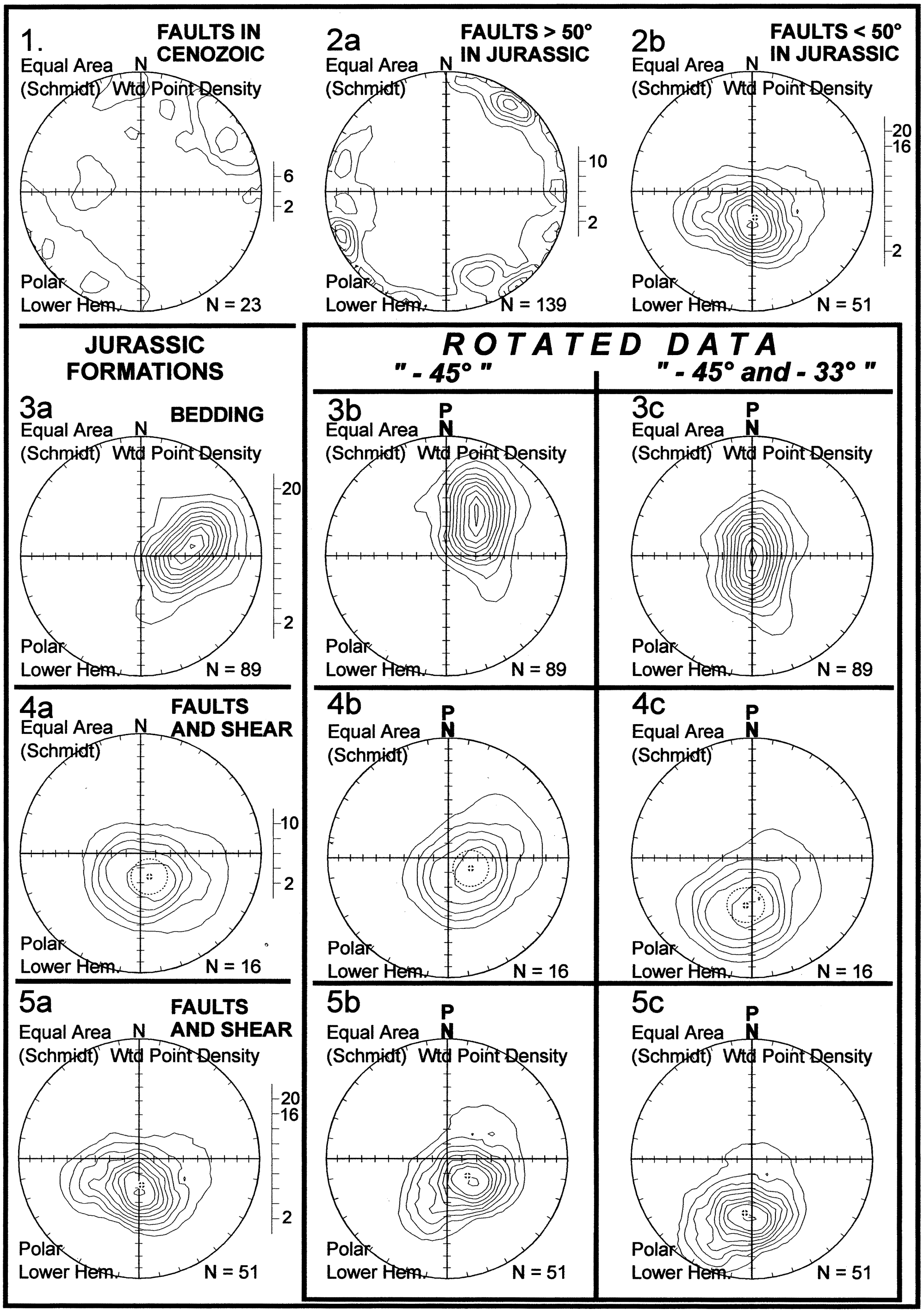

Palaeoenvironment: formation of the Komi Leibadi Mélange and the emplacement of the Pappades Ophiolite

The structure and the tectonostratigraphic position of the Komi Leibadi mélange identify it as a tectonic mélange (cf. Hsü 1974). Besides some of the radiolarite and greywacke, the components of the mélange represent various levels of an oceanic assemblage (Spray 1991). Mélange components of island arc provenance (pyroclastics, rhyolite, andesite) are lacking. Like the Pagondas Complex (Robertson 1991), the Komi Leibadi mélange is envisaged to have evolved in an intra-oceanic subduction zone along the sole of the overriding ophiolite nappe, a setting which was postulated by Simantov et al. (1991) for central Evvoia. The observed composition could have evolved stepwise, initially by offscraping and underplating of deeper-seated ultra basic and gabbroic substrates, followed by the subcretion of volcanic oceanic substrates, and finally of radiolarite and greywacke from the drowned Pelagonian substrate, thus reflecting the compositions along the basal décollement over which the ophiolite was transported (cf. case studies in Dewey 1976). Flow mélange, characterised by chaotic matrix supported block fabric (Cowan 1985), probably acted as a lubricant between the descending and overriding plates, whereby tectonic erosion of the base of the overriding ophiolite and erosion of the top of the ophiolite could also have added material to the mélange (Shreve and Cloos 1986; Dickinson 1995; Underwood and Moore 1995). In contrast to the Pagondas Mélange (Robertson 1991), limestones were neither accreted nor subcreted to the Komi Leibadi mélange, apparently because the Pappades Ophiolite composite nappe did not directly override carbonate formations.

Age constraints of ophiolite emplacement

The metamorphic ages determined by Spray and Roddick (1980) for amphibolites taken from the soles of numerous Hellenic ophiolites correspond to late Lower to early Middle Jurassic, the time of subcretion of the amphibolites to the sole of the ophiolites (cf. Woodcock and Robertson 1977; Spray and Roddick 1980; Spray et al. 1984; Robertson et al. 1991). This was the time of plate polarity change, from divergent sea-floor spreading to convergent intra-oceanic subduction and obduction. Final emplacement of the ophiolite occurred during latest Late Jurassic to earliest Early Cretaceous (Baumgartner and Bernoulli 1976), based on the age of the Achladi radiolarite, which together with the Megali Lakka greywacke is the substrate of the Komi Leibadi mélange.

Direction of tectonic emplacement of the oceanic formations with consideration of post-Eohellenic deformations

The tectonic analysis shows that the normal faults of the study area affected both the Cenozoic and Mesozoic formations, whereas low-angle shear and thrust faulting primarily affected the pre-Cretaceous formations (diagrams 1, 2a, 2b of Fig. 7). This distinguishes two dominant deformation eras: an Eohellenic deformation plan, characterised by thrust faults and low-angle shear; and a post-Eohellenic deformation plan, characterised by normal faults. The Eohellenic deformation, which is of interest in this context, is especially evident in the radiolarites as shear planes and in the serpentinites as thrust faults, and in the northern facies zone as imbrication in the contact zone between the radiolarite and the subjacent limestones of the Xiron Formation (Figs. 3, 4A). The pole diagrams (diagrams 4a and 5a of Fig. 7) show that the shear and thrust planes have predominantly S-vergence, indicating that thrusting was from the north. This agrees with a previous schematic tectonic reconstruction made by Katsikatsos (1976) for Evvoia, and in a regional context, is the prevalent Eohellenic thrust direction on the Argolis peninsula (Baumgartner 1985; Clift and Dixon 1998).

Numerous post-Eohellenic tectonic phases of uplift and subsidence, documented by laterites, rudistid limestones, molasse and intervening unconformities, have caused crustal rotations, some of which have altered the original bedding and (Eohellenic) thrust fault attitudes. Presently, the Pelagonian formations, including the rudistid limestones are tilted generally towards the WSW (Diagram 3a of Fig. 7). A reconstruction (Fig. 8) shows that strong uplift occurred in the Aegean realm during the post-Cretaceous Era, which apparently exhumed the Aegean metamorphic zone and subsequently led to the deposition of exotic Cenozoic molasse (Besenecker and Büttner 1978). This anti-form structure (Fig. 8) collapsed into graben and horst blocks (Fig. 4B), a process that is still going on in the Aegean shear zone (McKenzie and Jackson 1986). These episodes occurred as the Hellenides acquired an arcuate pattern, whereby northern Evvoia rotated clockwise approximately 26–45° (Fig. 1; Kissel and Laj 1988).

Corrections for the post-Cretaceous clockwise rotation of the Hellenides (diagrams 3b, 4b, 5b of Fig. 7; Kissel and Laj 1988), and for formation tilting (diagrams 3c, 4c, 5c of Fig. 7), restores a southeastward or, respectively, southward palaeo-thrust direction, indicating that the Pappades Ophiolite had a north or

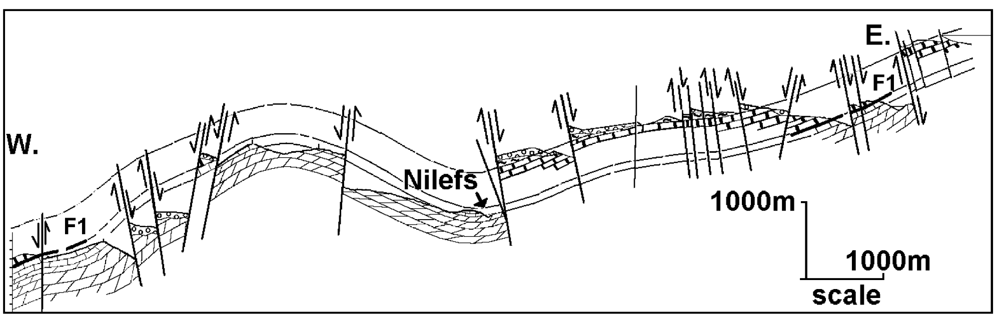

Fig. 8 Reconstructed post-Cretaceous E–W geological section. This reconstruction shows the Mesozoic formations after folding, westward tilting, and a relative uplift of approximately 3000 m toward the eastern margin of the study area. This deformation was accompanied by erosion and clastic deposition, and was followed by normal faulting (compare Fig. 4B and Diagram 1 of Fig. 7)

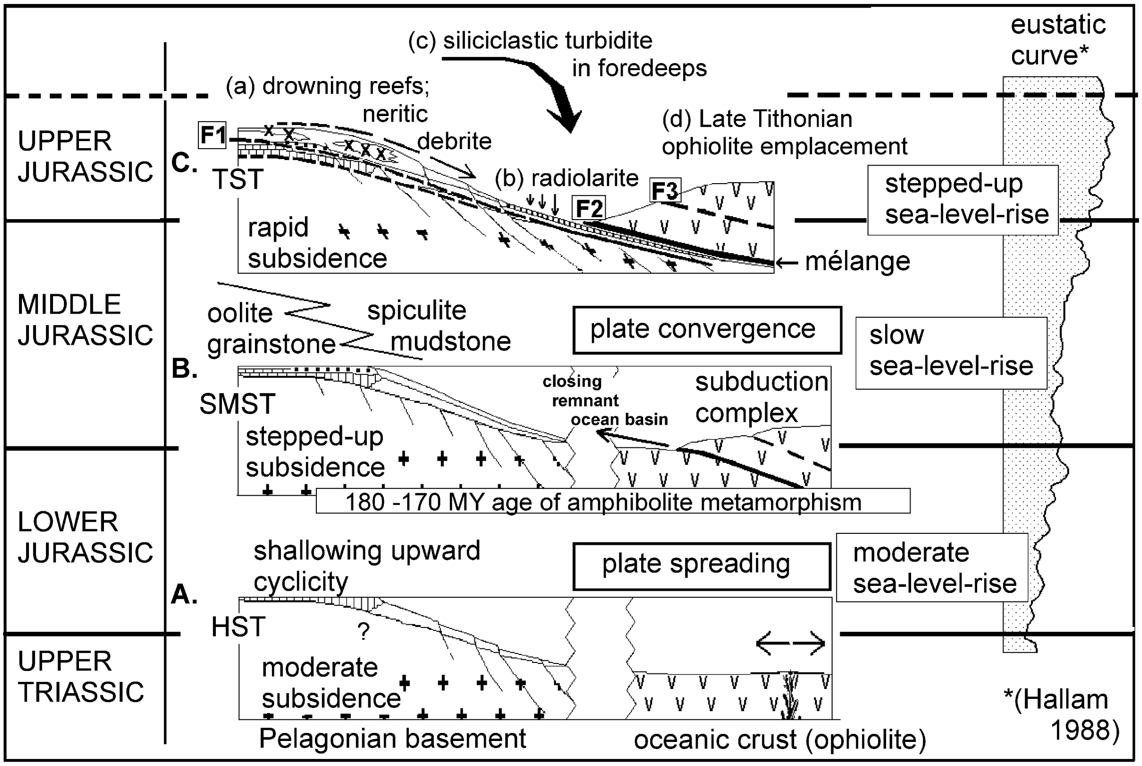

Fig. 9A–C The evolution of the Pelagonian margin in divergent, convergent and ophiolite emplacement settings and the interplay of carbonate accumulation, tectonic subsidence and second-order eustacy. **A** During the Late Triassic to Middle Jurassic, carbonate accumulation responded to moderate global sea-level rise (Jurassic eustatic curve after Hallam 1988) and tectonic subsidence in a divergent setting due to the formation of the Meliata-Vardar arm of the Neotethys (Stampfli and Mosar 1998), and constructed a prograding highstand systems tract (HST), characterised by shallowing upward cyclicity of the third to fifth order (cf. Figs. 3, 5). **B** During approximately the Early Jurassic/Middle Jurassic transition the change-over from plate spreading to plate convergence and a period of slowed-down sea-level rise began. This interim appears to have been a period of sedimentary equilibrium, in which a shelf margin systems tract (SMST) formed, culminating with a grainstone wedge with interdigitated spiculite mudstones. **B,C** The SMST was buried beneath a transgressive systems tract (TST), composed mainly of spiculites and nodular chert mudstones, as a response to stepped-up subsidence, probably due to the beginning of plate convergence and the subduction and closure of a remnant ocean basin, partially preserved in the Komi Leibadi mélange. **C** The tectonically induced subsidence and the stepped-up Late Jurassic sea-level rise, was initially conducive for reef accommodation, but inevitably led to reef drowning (a) and burial beneath sponge-spiculite muddy facies. Subsidence of the Pelagonian platform below the CCD is documented by a final succession of (a) neritic debrites, (b) radiolarites, and (c) distal siliciclastic turbidites. The advancing ophiolite telescoped outer-shelf facies over the inner peritidal realm (F1) and (d) emplaced the Nilefs ophiolite nappe, including the Komi Leibadi tectonic mélange, over the drowned shelf facies (F2). An intra-ophiolite thrust (F3) emplaced the Basilika nappe over the Nilefs nappe and its volcanic and pelagic sedimentary cover

northwestern derivation. This is in accord with the present facies analysis, showing that a deeper starved marine zone was situated towards the north during the Jurassic.

Discussion and conclusion

The evolution of the Pelagonian shelf and the overthrust oceanic formations in northern Evvoia

Late Triassic to Late Lower Jurassic

The initial Triassic scenario in the Hellenides (Stampfli et al. 1991), was one of extension and lithospheric thinning, which led to the opening of the Neotethys and to the subsidence of the passive margins (Fig. 9A). This early history is only fragmentarily documented in the study area by an Upper Triassic intraformational breccia (east of Ellinika; Figs. 2, 3, 4A), containing reefal debris. It is most likely a Late Triassic platform-slumping breccia (Robertson 1991). The reefal lithoclasts are envisaged to have stemmed from a slumping Pantokrator reef margin which was laterally equivalent to the Upper Triassic to late Lower Jurassic reef margin known from the Pantokrator progradational shelf of Hydra (Schäfer and Senowbari-Daryan 1982). Another contemporary progradational shelf, that also was initially dominated by an extensive peritidal environment like that of the study area and of Hydra, was the Othrys shelf, NW of the study area

(Smith et al. 1975). Like the shelf of the study area, the over 1600-m-thick peritidal formation of the Othrys shelf was laterally associated with a 200-m-thick nodular chert limestone succession, documenting a slumping passive margin, starved of sediment (Robertson 1991). These regional observations on early basin evolution compared with that of the study area – reef breccias, extensive peritidal formations and laterally associated nodular chert limestone – suggest that the Pelagonian shelf followed a similar evolution over a larger region. In the terminology of sequence stratigraphy (Sarg 1988; Van Wagoner et al. 1988), these Late Triassic and Lower Jurassic Pelagonian platform margins were high-stand systems tracts (HST) that prograded, while keeping pace with subsidence, and occasionally became exposed during subordinate eustatic fluctuations (Fig. 5).

The newly formed oceanic realm (Stampfli et al. 1998) adjacent to the Pelagonian micro-continent was the depositional basin of radiolarite (Elias Complex), which accumulated below the CCD on top of the pillow lavas of the Pappades Ophiolite assemblage. These radiolarites are envisaged to have formed in the early divergent oceanic setting at the same time that the Pelagonian HST was prograding; however, fossil evidence which could date these radiolarites is still lacking.

Late Lower and Middle Jurassic

Plate convergence is postulated to have begun, during the late Lower Jurassic (dating of amphibolite metamorphism: Spray and Roddick 1980; Spray et al. 1984), at which time second-order eustacy was relatively stable (Fig. 9B). During this changeover from divergent to convergent plate motion a temporary slowdown in the subsidence rate is suggested to have favoured the build-up of the shelf margin grainstone wedge that occurs at the top of the Pantokrator Formation and intercalates with nodular chert limestone (Fig. 3). In the context of sequence stratigraphy, this grainstone wedge is interpreted as a shelf margin systems tract (SMST; Figs. 3; 9B), that evolved over a type-2 sequence boundary ("... interpreted to form when the rate of eustatic fall is less than or equal to the rate of basin subsidence at the platform/bank margin...": Sarg 1988, p 156). This sequence boundary coincides with the substrate of the oolite wedge. The age range of the SMST is still insecure (Fig. 3).

In the oceanic Elias Complex, the change from radiolarite to pelagic carbonate deposition (Fig. 3) is interpreted to have been coeval with the changeover from divergent to convergent plate movement, and to have evolved in an intra-oceanic forearc subduction complex as the overriding plate lifted the oceanic substrate above the CCD (Fig. 9B).

Upper Jurassic

The deposition of hemipelagic nodular chert limestones over the antecedent SMST, during the ?Middle to early Late Jurassic, signals that shelf subsidence was occurring, which circumstantial evidence indicates was due to tectonic loading of the Pelagonian Margin by the advancing Pappades Ophiolite composite nappe and was enhanced by stepped-up second-order eustatic sea-level rise (Fig. 9C). Reef growth on the shelf terrace was initially accommodated by the increased rate of subsidence, but later, tectonically induced slumping led to reef drowning and rapid burial by deeper water facies (Figs. 3, 6, 9C). The drowning of the Pelagonian margin culminated with the intercalation of neritic debrites and radiolarian pelite in a below the CCD palaeoenvironment. Robertson (1991) suggests that a foredeep developed in front of the advancing ophiolite nappe, into which boulders were deposited, derived from antecedent formations exposed in fault escarpments. In the final depositional episode, siliciclastic turbidites (Megali Lakka greywacke) were deposited on top of the radiolarite, parallel to the shelf (Figs. 2, 3). The turbidites are interpreted as distal synorogenic flysch, derived from uplifted Pelagonian basement which may have become exposed by sequential collision of oceanic crust (Eohellenic ophiolite) with the Pelagonian continental margin, much like the present situation in the Huon Gulf, Papua New Guinea (Ingersoll et al. 1995; Dickinson 1995). The turbidites were deposited during approximately the Late Tithonian before the Pappades Ophiolite was emplaced, an age constraint supported by the Tithonian (or younger) age of the debris limestones (Table 1), which intercalate with the lower Achladi radiolarite (Fig. 6).

The Nilefs and Basilika ophiolite nappes, and interleaved Elias Complex, are interpreted as imbricate slabs of a subduction wedge of a forearc subduction complex, comparable to the Recent scenario of the New Britain trench, where an oceanic subduction complex is being thrust over the Solomon Sea remnant ocean towards the Papua New Guinea shelf (cf. Huon Gulf; Ingersoll et al. 1995; Dickinson 1995).

The Komi Leibadi mélange and the entire complex of telescoped Pelagonian and oceanic formations (F1, F2, F3; Figs. 4A, 9C) may represent a juvenile stage of an accretionary complex, which perhaps would have evolved into a Pagondas-type accretionary complex (Robertson 1991) had nappe thrusting continued. However, it is supposed that obduction came to a premature halt in the study area for the following possible reasons: in addition to the resistance that the relative buoyant Pelagonian continental crust must have presented to subduction (Dewey 1976), irregularities of the collisional margin could have promoted thrusting of different intensities from place to place (Ingersoll et al. 1995). Shelf telescoping along thrust F1 and along a possible deeper décollement, coinciding with the broken formation that often occurs at the base of the Pantokrator Dolomite (Fig. 4A,B), may have translated most of the thrust energy.

The provenience of the Pappades Ophiolite

The tectonic analysis, in consideration of post-Eohellenic rotations, indicates that the Pappades Ophiolite had a derivation northwards of the study area. Regional palaeogeographic reconstructions (Kissel and Laj 1988; Stampfli et al. 1991) show that the Vardar ocean was located north of the Pelagonian zone during the Late Jurassic and that it closed (Stampfli and Mosar 1998) at the same time that the Eohellenic ophiolite of Pappades was emplaced. Although this circumstantial evidence strongly supports previous Vardar-root models (Bernoulli and Laubscher 1972; Jacobshagen et. al. 1976; Zimmerman and Ross 1976; Jacobshagen et al. 1978b), the regional palaeogeography still remains controversial (Scherreiks 1998b; Clift 1998).

Acknowledgements The author gratefully acknowledges the financial support of the "Geologische Staatssammlung" of the state of Bavaria, and thanks are given to the following persons for their support: H. Miller ("Geologische Staatssammlung and Institut für Allgemeine und Angewandte Geologie," Ludwig Maximillian University of Munich), I. Fruth ("Geologische Staatssammlung"), G. Pappadeas (IGME, Athens), O. Ebli and F. Schlagintweit ("Institut für Paläontologie und Historische Geologie", Munich); and members of the above institutions for technical assistance: L. Böck, S. Gräler, A. Gretz, B. Sommer, M. Werner and H. Voecks. Special thanks are given to L. Bäsmann-Scherreiks, Georgos and Silvia Violakis, Kostas and Heleni Koukoutsis, Jürgen and Marianne Nikolai. For critical reviews of the original manuscript, thanks are given to S. Van Rose (Geoventures, London) and H. Bahlburg, S. Dürr, V. Jacobshagen, A. H. F. Robertson and an anonymous reviewer.

References

Anonymous (1972) Penrose field conference on ophiolites. Geotimes 17 : 24–25

Aubouin J (1959) Contribution à l'étude géologique de la Grèce septentrionale: les confins de l'Epire et de la Thessalie. Ann Géol Pays Hellén 10 : 1–484

Aubouin J (1965) The Hellenides. In: Aubouin J (ed) Developments in Geotectonics, vol 1. Geosynclines. Elsevier, Amsterdam, pp 43–67

Aubouin J, Guernet Cl (1964) Sur la stratigraphie et la téctonique de l'Eubée moyenne (Gréce). Bull Soc Géol France 5 : 821–827

Bachmann GH, Risch H (1979) Die geologische Entwicklung der Argolis Halbinsel (Peloponnes, Griechenland). Geol Jahrb 32 : 3–177

Badiozamani K (1973) The Dorag dolomitization model: application to the Middle Ordovician of Wisconsin. J Sediment Petrol 43 : 965–984

Bannert D, Bender H (1968) Zur Geologie der Argolis-Halbinsel (Peloponnes, Griechenland). Geol Paleontol 2 : 151–162

Bassoulet JP, Guernet C (1970) Le trias et le jurassique de la région des lacs de Thèbes (Béotie et Locride, Grèce). Rev Micropaléontol 12 : 209–217

Baumgartner PO (1985) Jurassic sedimentary evolution and nappe emplacement in the Argolis peninsula (Peloponnesus, Greece). (Denkschr Schweiz Naturforsch Gesell 99) Birkhäuser, Basel

Baumgartner PO, Bernoulli D (1976) Stratigraphy and radiolarian fauna in a Late Jurassic–Early Cretaceous section near Achladi, Evvoia, eastern Greece. Eclogae Geol Helv 69 : 601–626

Bèbien J, Ohnenstetter D, Ohnenstetter M, Vergely P (1980) Diversity of Greek ophiolites: birth of oceanic basins in transcurrent systems. Ofioliti Spec Issue Tethyan Ophiolites 2 : 129–197

Besenecker H, Büttner D (1978) Late Cenozoic sediments on the islands between Euboea and Turkey. In: Closs H, Roeder D, Schmidt K (eds) Alps, Apennines, Hellenides. Schweizerbart, Stuttgart, pp 502–506

Bernoulli D, Laubscher H (1972) The palinspastic problem of the Hellenides. Eclogae Geol Helv 65 : 107–118

Bernoulli D, Renz O (1970) Jurassic carbonate facies and new ammonite faunas from western Greece. Eclogae Geol Helv 63 : 573–607

Bignot G, Fleury JJ, Guernet C (1971) Sur la stratigraphie du Crétacé supérieur et du flysch en Eubée moyenne (zone pélagonienne, Gréce). Bull Soc Géol France 13 : 484–489

Bosence D, Wood J, Rose T, Quing H (1999) Low- and high-frequency sea-level changes control peritidal carbonate cycles, facies and dolomitization in the rock of Gibraltar (Early Jurassic, Iberian Peninsula). J Conf Absr 4/2, Cambridge Publ : 904

Capedri S (1974) Genesis and evolution of a typical alpine-type peridotite mass under deep-seated conditions (Central Euboea, Greece). Boll Soc Geol Ital 93 : 81–114

Celet P (1962) Contribution à l'etude geólogique du Parnasse-Kiona et d'une partie des région méridionale de la Grèce continentale. Ann Géol Pays Hellén 13 : 1–446

Chenevart C, Katsikatsos G (1967) Geological map of the island of Evvoia 1 : 200,000. Inst Geol Subsurface Res, Athens

Cita MB (1965) Jurassic, Cretaceous and Tertiary microfacies from the southern Alps (northern Italy). Int Sediment Petrogr Ser (VIII). Brill, Leiden

Clift PD (1998) On the origin of some Eohellenic ophiolites (Reply). Eclogae Geol Helv 91 : 432–434

Clift PD, Dixon JE (1998) Jurassic ridge collapse, subduction initiation and ophiolite obduction in the southern Greek Tethys. Eclogae Geol Helv 91 : 123–138

Cowan DS (1985) Structural styles in Mesozoic and Cenozoic melanges in the western Cordillera of North America. Bull Geol Soc Am 96 : 451–462

Dercourt J (1972) The Canadian cordillera, the Hellenides and the sea floor Spreading theory. Can J Earth Sci 9 : 709–743

Dercourt J, Makris J, Melidonis N (1980) Grèce. Introduction à la géologie générale. Twenty-sixth Congr Géol Int Livret-Guide G12, Paris, 159 pp

Dewey JF (1976) Ophiolite obduction. Tectonophysics 31 : 93–120

Dickinson RW (1995) Forearc basins. In: Busby CJ, Ingersoll RV (eds) Tectonics of sedimentary basins. Blackwell, Oxford, pp 221–261

Dunham R J (1971) Meniscus cement. In: Bricker OP (ed) Carbonate cements. Johns Hopkins Press, Baltimore, pp 297–300

Ferrière J, Bertrand J, Simantov J, Wever P de (1989) Comparaison entre des formations volcanodetritiques ("Mélanges") du Malm des Hellènides internes (Othrys, Eubée. Implications Géodynamique. Bull Geol Soc Greece 20 : 223–235

Fischer AG (1986) Climatic rhythms recorded in strata. Ann Rev Earth Planet Sci 14 : 351–376

Flügel E (1974) Fazies-Interpretation der *Cladocoropsis*-Kalke (Malm) auf Karaburun, W-Anatolien. Arch Lagerstforsch (Ostalpen) Sonderbd 2, Leoben, pp 79–94

Flügel E (1982) Microfacies analysis of limestones. Springer, Berlin Heidelberg New York

Flügel E (1983) Mikrofazies der Pantokrator-Kalke (Lias) von Korfu, Griechenland. Facies 8:263–300

Folk RL (1965) Petrology of sedimentary rocks. Hemphills, Austin, Texas

Folk RL, Land LS (1975) Mg/Ca ratio and salinity, two controls over crystallization of dolomite. Bull Am Assoc Petrol Geol 59:60–68

Guernet Cl (1965) Formations éruptives anté jurassiques en Eubée moyenne. Bull Soc Géol France 7:56–68

Guernet Cl (1971) Etudes géologiques en Eubée et dans les regions voisines (Grèce). Thèse d'Etat Univ Paris, Paris

Guernet Cl, Parrot JF (1972) Le cortège ophiolitique de l'Eubée moyenne (Gréce): position et relations avec les séries mésozoiques. Cah OSTROM Sér Géol 4, Bondy, pp 67–75

Guernet Cl, Robert P (1973) Sur l'existence de bauxites d'age jurassique en Eubée (Gréce). CR Acad Sci Paris 276:885–887

Grotzinger J P (1986) Cyclicity and paleoenvironmental dynamics, Rocknest platform, northwest Canada. Bull Geol Soc Am 97:1208–1231

Hallam A (1988) A re-evaluation of Jurassic eustacy in the light of new data and the revised Exxon curve. In: Wilgus CK, Hastings BS, Kendall CGStC, Posamentier HW, Ross CA, Wagoner J van (eds) Sea-level changes: an integrated approach. Soc Econ Paleontol Mineral Spec Publ 42:261–273

Hanshaw BB, Back W, Dieke RG (1971) A geochemical hypothesis for dolomitization by groundwater. Econ Geol 66:710–724

Hanzawa S (1961) Facies and micro-organisms of the Paleozoic, Mesozoic and Cenozoic sediments of Japan and her adjacent islands. Int Sediment Petrogr Ser V. Brill, Leiden

Hashimoto W (1960) Stromatoporids from the Ainonai limestone, Kitami province, Hokkaido. Sci Rep Tokyo Kyoiku Daigaku Sect C 65:195–203

Hsü KJ (1974) Melanges and their distinction from olistostromes. In: Dott RH, Shaver RH (eds) Modern and ancient geosynclinal sedimentation. Soc Econ Paleontol Mineral Spec Publ 19:321–333

Hudson RGS (1953) The systematic position of the Mesozoic Stromatoporid *Cladocoropsis* Felix 1907 Ann Mag Nat Hist 68:615–619

Hudson RGS (1955) Sequanian stromatoporids from south-west Arabia. Note Mém Moyen Orient 6:234–239

Humphrey JD (1988) Late Pleistocene mixing-zone dolomitization, southeastern Barbados, West Indies. Sedimentology 35:327–348

Hynes J, Nisbet EG, Smith AG, Welland MJP, Rex DC (1972) Spreading and emplacement ages of some ophiolites in the Othrys region (eastern central Greece). Z Dtsch Geol Ges 123:455–468

Ingersoll RV, Busby CJ (1995) Tectonics of sedimentary basins. In: Busby CJ, Ingersoll RV (eds) Tectonics of sedimentary basins. Blackwell, Oxford, pp 1–51

Ingersoll RV, Graham SA, Dickinson RW (1995) Remnant ocean basins. In: Busby CJ, Ingersoll RV (eds) Tectonics of sedimentary basins. Blackwell, Oxford, pp 363–391

Jacobshagen V (1986) Geologie von Griechenland. Bornträger, Berlin

Jacobshagen V, Risch H, Roeder D (1976) Die eohellenische Phase, Definition und Interpretation. Z Dtsch Geol Ges 127:133–145

Jacobshagen V, Dürr S, Kockel F, Kopp KO, Kowalczyk G (1978a) Structure and geodynamic evolution of the Aegean region. In: Closs H, Roeder D, Schmidt K (eds) Alps, Apennines, Hellenides. Schweizerbart, Stuttgart, pp 537–564

Jacobshagen V, Skala W, Wallbrecher E (1978b) Alpine structure and development of the southern Pelion Peninsula and the North Sporades. In: Closs H, Roeder D, Schmidt K (eds) Alps, Apennines, Hellenides. Schweizerbart, Stuttgart, pp 484–488

Jones G, De Wever P, Robertson AHF (1992) Significance of radiolarian age data to the Mesozoic tectonic and sedimentary evolution of the northern Pindos Mountains, Greece. Geol Mag 129:385-400

Katsikatsos G (1976) La structure tectonique d'Attique et de l'ile d'Eubée. Bull Soc Géol France 19:211–228

Katsikatsos G (1977) L'Eubée centrale. Bull Soc Géol France 19:108–110

Katsikatsos G, Fytikas M, Koukis G (1969) The iron-nickel-ore deposits of the northeastern sector of central Euboea–Kimi region. Geol Reconnaissance Rep 45:1–89

Katsikatsos G, Kounis G, Fytikas M (1975) On the magnesite deposits of the Papadhes-Vassilika area. Mineral Deposits Res, vol 5. Inst Geol Mineral Res, Athens, pp 1–86

Katsikatsos G, Kounis G, Fytikas M, Mettos A, Vidakis M (1980) Geological map of Greece, Limni Sheet 1:50,000. IGME Publ Dept, Athens

Katsikatsos G, De Bruijn H, Van der Meulen AJ (1981) The Neogene of the island of Euboea (Evia): a review. Geol Mijnb 60:509–516

Katsikatsos G, Mettos A, Vidakis M (1984) Geological map of Greece, Istiea Sheet 1:50,000. IGME Publ Dept, Athens

Katsikatsos G, Migiros MT, Mettos A (1986) Geological structure of internal Hellenides (E. Thessaly–SW Macedonia, Euboea–Attica–northern Cyclades Islands and Lesvos). Geol Geophys Res Spec Issue IGME, Athens, pp 191–212

Kelts K, McKenzie J (1984) A comparison of anoxic dolomite from deep-sea sediments: Quaternary Gulf of California and Messinian Tripoli Formation of Sicily. In: Garrison RE, Kastner M, Zenger DH (eds) Dolomites of the Monterey Formation and other organic-rich units. Publ Soc Econ Paleontol Mineral Pacific Sect 41:119–140

Kissel C, Laj C (1988) The Tertiary geodynamical evolution of the Aegean arc: a paleomagnetic reconstruction. Tectonophysics 146:183–201

Kurzweil H (1966) Zur Mineralogie Ni-führender Verwitterung- und sedimentärer Eisenerze in Lokris, Mittelgriechenland. Berg Hüttenmänn Mh Montan Hochsch Leoben 111:488–497

Land LS (1973) Contemporaneous dolomitization of middle Pleistocene reefs by meteoric water, north Jamaica. Bull Mar Sci 23:64–92

Lavoie D (1995) Hot vent chemosynthetic bacterial community in Ordovician Ophicalcites, Quebec Appalachians, Canada. In: Bosence D (ed) Abstr 10 Bathurst Meeting of Carb Sedimentol, Royal Holloway, University of London, p 36

McKenzie D, Jackson J (1986) A block model of distributed deformation by faulting. J Geol Soc Lond 143:349–353

Melidonis N (1960) The nickeliferous iron ore deposits of Artaki-Politikon Verturon. IGSR Geol Reconnaissance Rep 32, Athens, pp 1–27

Mercier J (1966) Paléogéographie, orogenèse, métamorphisme et magmatisme des Zones internes des Hellénides en Macédoine (Gréce) vue d'ensemble. Bull Soc France 8:1020–1049

Mercier J, Vergely P (1972) Les mélanges ophiolitiques de Macédoine (Grèce): décrochement d' âge anté-crétacé supérieur. Z Dtsch Geol Ges 123:469–489

Monty CLV (1981) Spongiostromate vs. Porostromate stromatolites and oncolites. In: Monty CLV (ed) Phanerozoic stromatolites 1–4. Springer, Berlin Heidelberg New York

Moore RC (ed) (1964) Treatise on invertebrate paleontology, part C, Protista. Univ Kansas Press, Topeka

Mountrakis D, Sapountzis E, Kilias A, Eleftheriadis G, Christofides G (1983) Paleogeographic conditions in the western Pelagonian margin in Greece during initial rifting of the continental area. Can J Earth Sci 20:1673–1681

Mullins HT, Wise SW, Gardulski AF, Hinchey EJ, Masters PM, Siegel DI (1985) Shallow subsurface diagenesis of Pleistocene periplatform ooze: northern Bahamas. Sedimentology 32:473–494

Mutti E, Crombelli G, Pozzi R (1970) Geological studies on the Dodecanese Islands (Aegean Sea). Ninth geological map of the island of Rhodos (Greece) explanatory notes. Ann Géol Pays ellén 22 : 77–226

Ori GG, Friend PF (1984) Sedimentary basins formed and carried piggyback on active thrust sheets. Geology 12 : 475–478

Pangaea Scientific (1998) Spheri Stat 2 for Windows 3.1 version 2.2 Users' Manuel. Brockville, Ontario pp 240

Parrot JF, Guernet Cl (1972) Le cortège ophiolitique de l'Eubée moyenne (Grèce): Étude pétrographique des formations volcaniques et des roches métamorphiques associées dans les monts Kandilis aux radiolarites. Cah OSTROM Sér Géol 4 : 153–161

Partsch J (1887) Die Insel Korfu. Eine geographische Monographie. Petermanns Mitt Ergänzungsband 1988, 4, Justus Perthes, Gotha

Perconig E (1968) Microfacies of the Triassic and Jurassic sediments of Spain. Int Sediment Petrogr Ser X. Brill, Leiden

Petrascheck WE (1961) Zur Bildung griechischer Magnesitlagerstätten. Radex Rundsch 4 : 641–646

Plint AG, Eyles N, Eyles C, Walker RG (1992) Control of sea level change. In: Walker RG, James NP (eds) Facies models. Geol Assoc Canada, St. John's, pp 15–25

Pratt BR, James NP, Cowan A (1992) Peritidal carbonates. In: Walker RG, James NP (eds) Facies models. Geol Assoc Canada, St. John's, pp 303–322

Renz C (1940) Die Tektonik der griechischen Gebirge. Pragm Akad 8, Athens, pp 1–171

Renz C (1955) Die vorneogene Stratigraphie der normalsedimentären Formationen Griechenlands. Inst Geol Subsurface Res, Athens

Rimpel K, Rothenhöfer H (1983) Stratigraphie und Tektonik der Toufa Decke und ihres Unterlagers (Parnass-Kiona-Zone, Helleniden). Z Dtsch Geol Ges 134 : 467–481

Robertson AHF (1991) Origin and emplacement of an inferred Late Jurassic subduction–accretion complex, Euboea, eastern Greece. Geol Mag 128 : 2–41

Robertson AHF, Clift PD, Degnan PJ, Jones G (1991) Palaeogeographic and palaeotectonic evolution of the eastern Mediterranean Neotethys. Palaeogeogr Palaeoclimatol Palaeoecol 87 : 289–343

Sarg JF (1988) Carbonate sequence stratigraphy. Soc Econ Paleontol Mineral Spec Publ 42 : 155–182

Sartoni S, Crescenti U (1962) Recerche biostratigrafiche nei Mesozoic dell'Appenino meridionale. Giorn Geol 29 : 161–304

Schäfer P, Senowbari-Daryan B (1982) The Upper Triassic Pantokrator Limestone of Hydra (Griechenland): an example of a prograding reef complex. Facies 6 : 147–164

Scherreiks R (1998a) The evolution of a passive margin in response to plate tectonics, eustacy, and an advancing ophiolite nappe (Jurassic, NE-Evvoia, Greece). Terra Nostra 98 : 72–73

Scherreiks R (1998b) On the origin of some Eohellenic ophiolites (Commentary). Eclogae Geol Helv 91 : 431–432

Schulz M, Schäfer-Neth C (1997) Translating Milankovitch climate forcing into eustatic fluctuations via thermal deep water expansion: a conceptual link. Terra Nova 9 : 228–231

Shreve RL, Cloos M (1986) Dynamics of sediment subduction, melange formation, and prism accretion. J Geophys Res 91 : 10229–10254

Sibley DF (1982) The origin of common dolomite fabrics. J Sediment Petrol 52 : 1087–1100

Sibley DF, Gregg JM (1987) Classification of dolomite rock texture. J Sediment Petrol 57 : 967–975

Simantov J, Bertrand J (1987) Major and trace element geochemistry of the Central Euboea basaltic rocks (Greece). Possible geotectonic implications. Ofioliti 12 : 201–218

Simantov J, Economou C, Bertrand J (1991) Metamorphic rocks associated with the Central Euboea ophiolite (southern Greece): some new occurrences. In: Malpus J, Moores EM, Panayiotou A, Xenophontos C (eds) Ophiolites, oceanic crustal analogies. Proc Symp Troodos 1987, Geol Surv Dept Nicosia/Cyprus, pp 285–293

Sloss LL (1963) Sequences in the cratonic interior of North America. Bull Geol Surv Am 74 : 93–114

Smith AG, Hynes AJ, Menzies M, Nisbet EG, Price I, Welland MJP, Ferriére J (1975) The stratigraphy of the Othris mountains, eastern central Greece: a deformed Mesozoic continental margin sequence. Eclogae Geol Helv 68 : 463–481

Smith AG, Woodcock NH, Naylor MA (1979) The structural evolution of a Mesozoic continental margin, Othris Mountain, Greece. J Geol Soc Lond 136 : 589–603

Spiliadis T (1977) Die Verbreitung von Nickelhaltigen Eisenerzen auf Euböa, Griechenland. Erzmetall 30 : 313–316

Spray JG (1991) Structure of the ocean crust as deduced from ophiolites. In: Floyd PA (ed) Oceanic basalts. Blackie, Glasgow, pp 49–62

Spray JG, Roddick JC (1980) Petrology and ^{4039}Ar geochemistry of some Hellenic subophiolite metamorphic rocks. Contrib Mineral Petrol 72 : 43–55

Spray JG, Bebien J, Rex DC, Roddick JC (1984) Age constraints on the igneous and metamorphic evolution of the Hellenic–Dinaric ophiolites. Geol Soc Lond Spec Publ 17 : 619–627

Stampfli G, Mosar J (1998) The plate tectonics of the western Tethyan regions. Terra Nostra 98 : 74–75

Stampfli G, Marcoux J, Baud A (1991) Tethyan margins in space and time. Palaeogeogr Palaeoclimatol Palaeoecol 87 : 373–409

Turnsek D, Barbulescu A (1969) Upper Jurassic Hydrozoa in central Dobrogea (Romania). Geologija 12 : 73–84

Turnsek D, Buser S, Ogorelec B (1981) An Upper Jurassic Reef complex from Slovenia, Yugoslavia. In: Toomey DF (ed) European fossil reef models. Soc Econ Paleontol Mineral Spec Pub 30 : 361–370

Underwood MB; Moore GF (1995) Trenches and trench-slope basins. In: Busby CJ, Ingersoll RV (eds) Tectonics of sedimentary basins. Blackwell, Oxford, pp 179–219

Van Wagoner JC, Posamentier HW, Mitchum RM Jr, Vail PR, Sarg JF, Loutit TS, Hardenbol J (1988) An overview of the fundamentals of sequence stratigraphy and key definitions. Soc Econ Paleontol Mineral Spec Publ 42 : 39–45

Ward WC, Halley RB (1985) Dolomitization in a mixing zone of near seawater composition, late Pleistocene, northeastern Yucatan Peninsula. J Sediment Petrol 55 : 407–420

Woodcock NH, Robertson AHF (1977) Origins of some ophiolite-related metamorphic rocks of the “Tethyan” belt. Geology 3 : 373–376

Zimmerman J (1972) Emplacement of the Vournos ophiolitic complex, northern Greece. Mem Geol Soc Am 132 : 225–239

Zimmerman J, Ross JV (1976) Structural evolution of the Vardar root zone, northern Greece. Bull Geol Soc Am 87 : 1547–1550